

1 **An experimental investigation of wide distillation fuel based on CTL on the**
2 **combustion performance and emission characteristics from a CI engine**

3

4 Yi Sun ^a, Wanchen Sun ^{a*}, Liang Guo ^a, Hao Zhang ^a, Yuying Yan ^b, Wenpeng Zeng ^a, Shaodian Lin ^a

5 ^a *State Key Laboratory of Automotive Simulation and Control, Jilin University, Changchun 130025,*
6 *China*

7 ^b *Faculty of Engineering, the University of Nottingham, Nottingham, UK, NG7 2RD*

8

9 **Abstract**

10 Coal to liquid (CTL) has promising application prospects as alternative diesel fuel, but the direct
11 application of coal-based synthetic diesel with high cetane number (CN) in compression ignition
12 (CI) engines also has problems. Therefore, the CTL is blended with gasoline to adjust the
13 physicochemical properties of the fuel, which is necessary to meet the requirements of efficient and
14 clean combustion. From the perspective of fuel design and combustion boundary condition control,
15 the effects of CTL/gasoline blends on the combustion performance and emission characteristics in
16 a CI engine are investigated in this study. Meanwhile, the variation in the start of injection (SOI)
17 along with the addition of exhaust gas recirculation (EGR) permits achieving clean combustion with
18 CTL/gasoline blends. Experimental results present that adding gasoline to CTL forms wide

* Corresponding author, Address for correspondence: State Key Laboratory of Automotive Simulation and Control, Jilin University, Changchun 130025, People's Republic of China.

E-mail address: sunwc@jlu.edu.cn (Wanchen Sun).

19 distillation fuel (WDF), which is conducive to reducing the required mixing timescale and
20 lengthening the chemical preparation timescale. CTL/gasoline blends bring in a higher premixed
21 combustion ratio (PCR) and keep NO_x and soot emissions at the lowest level after introducing EGR.
22 Simultaneously, the inhibition effects of CTL/gasoline blends on particulates' emissions are
23 apparent with or without EGR due to prolonged ignition delay (ID) and improved quality fuel-air
24 mixture, and the particulate mass of CG60 is significantly reduced by above 90% compared to pure
25 CTL. In addition, the CTL/gasoline blends show refined engine characteristics for broad SOI, and
26 the addition of gasoline to CTL is valid to alleviate the deterioration of combustion processes and
27 emissions caused by EGR. Coupling EGR and gasoline addition is an effective way to break the
28 trade-off relationship between NO_x and particulates' emissions for CTL.

29

30 *Keywords:* Coal to liquid; Wide distillation fuel; Combustion process; Particulate mode; Pollutant
31 emissions

32

33 **Highlights:**

- 34 ● CTL with high reactivity is not conducive to improving PCR and it is susceptible to EGR.
- 35 ● The CTL/gasoline blends as WDF suppress particles' emissions and promote the shifting of
36 particles towards smaller sizes.
- 37 ● The CTL/gasoline blends are beneficial to enhance the tolerance of the combustion processes
38 and emissions results to EGR.
- 39 ● Coupling EGR and gasoline addition is an effective way to break up the trade-off relationship
40 between NO_x and particulates' emissions for pure CTL.

Abbreviations			
AHRR	Apparent heat release rate	FTS	Fischer-Tropsch synthesis
AMP	Accumulation mode particle	IMEP	Indicated specific fuel consumption
ATDC	After top dead center	ISFC	Indicated specific fuel consumption
BTDC	Before top dead center	NMP	Nucleation mode particle
CA	Crank angle	SHC	Specific heat capacity
CD	Combustion duration	SOI	Start of injection
CI	Compression ignition	PCR	Premixed combustion ratio
CN	Cetane number	NMP	Nucleation mode particle
CTL	Coal to liquid	TDC	Top dead center
ECU	Electronic control unit	WDF	Wide distillation fuel
EGR	Exhaust gas recirculation		

42 **1. Introduction**

43 The internal combustion engines (ICEs) have been undergoing innovation and development since
 44 their birth, continuously promoting the progress of the global economy [1-3]. Applying an
 45 electronically controlled high-pressure common-rail injection system permits independent control
 46 of pressure establishment and mass of fuel injection, so the flexible adjustment of the boundary
 47 conditions in the compression ignition (CI) engine is achieved to acquire better performance and
 48 fuel economy. Therefore, the CI engine has a relatively wide application field as power machinery,
 49 especially in industry, agriculture, and transportation. In the face of schemed severe legislation on
 50 emissions, there is still challenging to break up the trade-off relation between NO_x and soot

51 emissions of diesel engines on account of mixing-controlled combustion [4-6]. The reason for this
52 phenomenon is that the conventional combustion process for the CI engine creates the locally
53 uneven distribution of the mixture and temperature in the cylinder: the high initial temperature of
54 flame is surrounded by excess air leading to NO_x generation while fuel spray is wrapped by high
55 temperature flame leading to soot formation [7, 8]. Although many manufacturers are trying to equip
56 vehicles with advanced after-treatment systems, these complex systems increase costs and cannot
57 solve the fundamental contradiction. Therefore, advanced combustion concepts and technologies
58 have become the hope of breaking through emission limitations, and the demands for pollutants
59 reduction accompanied by higher thermal efficiency compel the researchers to develop superior
60 combustion strategies as soon as possible. Aiming to overcome poor air-fuel mixing, it is the future
61 trend to actively introduce the premixed combustion mode into CI engines. These new combustion
62 concepts are classified into low-temperature combustion (LTC) [9], including homogeneous charge
63 compression ignition (HCCI) [10], premixed charge compression ignition (PCCI) [11], and reactive
64 controlled compression ignition (RCCI) [12] as representatives. The typical LTC adopts the ultra-
65 high injection pressure and heavy EGR to promote the premixed combustion [13, 14], which is
66 aimed at keeping the local combustion temperature sufficiently low and reduce the local fuel-rich
67 area in the cylinder to maintain the low level of emissions.

68 More importantly, energy has always been a prerequisite for human civilization, so petroleum
69 resources are vital to society's economic growth and sustainable development [15, 16]. Liquid fossil
70 fuels are still the main supply for ICEs as an energy source due to their high energy per unit density
71 and facilitation of storage and transportation, so there is a contradiction between the shortage of
72 fossil fuels and the growing demand for the energies. In allusion to the severe global energy

73 problems [17-19], searching for new alternative fuels has gradually attracted people's attention [20,
74 21], such as hydrogen energy, biomass fuels, and synthetic fuels, which have the potential to be
75 suitable for existing ICEs [22-26]. Meanwhile, it is essential to develop an energy diversification
76 strategy based on the local resource structure to secure the national energy supply. Coal to Liquid
77 (CTL), which uses coal as raw material, has been commercialized in countries with abundant coal
78 reserves, providing a practical approach to solving the oil supply problem with domestic coal
79 resources, such as South Africa, Indonesia, and China [27-30]. For the above countries with
80 relatively high coal consumption, it is strategic to apply CTL through Fischer-Tropsch synthesis
81 (FTS) technology to ensure clean and efficient coal utilization and guarantee energy security [31-
82 33]. The FT chemical processing as an indirect conversion path [34] makes the various natural
83 resources (such as coal, natural gas, and biomass) converted into intermediate gas products firstly,
84 and then above intermediate gas products are transformed into liquid hydrocarbon fuel [35].
85 Simultaneously, the CTL as the FTS product is designed to meet or exceed the required
86 specifications of commercial diesel [36, 37]. As a high-quality and clean alternative diesel fuel, CTL
87 with a high cetane number (CN) is mainly composed of saturated alkanes, and it is basically free of
88 sulfur and aromatic compounds. Because of the desirable properties of CTL, it can be used directly
89 or blended with traditional diesel in any proportion to reduce dependence on fossil fuels, and lower
90 fuel consumption also can be found by CTL [38-40]. Many researchers have proven that FT fuels
91 have broad application prospects as a promising alternative fuel for CI engines [31-36]. It is
92 demonstrated that the application of CTL as an alternative fuel not only has a positive effect on
93 traditional pollutants from CI engines, such as total hydrocarbons (HC), carbon monoxide (CO),
94 nitrogen oxides (NO), and particulate matter (PM) [41, 42], but also produces lower unregulated

95 emissions (formaldehyde, acetaldehyde, and ozone formation potential) than diesel [43, 44].
96 Valentin Soloiu et al. did the research employing a Box-Behnken design matrix to investigate the
97 correlation between thermal characteristics of Fischer-Tropsch coal-to-liquid fuel in relation to low
98 temperature heat release (LTHR), ignition delay, and combustion delay within the negative
99 temperature coefficient region (NTC) [45]. Vicente Bermúdez et al. tested gaseous emissions and
100 fuel consumption with five different fuels in a light-duty diesel engine with EURO IV, and it
101 concluded that the use of FT fuel causes lower regulated and unregulated emissions and fuel
102 consumption than diesel [43]. The reduction in carbonyl compound emissions was evaluated by Bin
103 Hao et al. using diesel engines running on FT diesel fuel synthesized from coal (CFT), and the result
104 showed that the use of CFT resulted in a remarkable reduction in carbonyl emissions and ozone
105 formation potential of the carbonyl compounds present in comparison with using diesel fuel [44].
106 An FT fuel has been experimented using a light-duty diesel engine under the New European Driving
107 Cycle (NEDC) by O Armas et al. [46], and there are noticeable reductions in THC, CO, and particle
108 mass compared to conventional diesel. Furthermore, extensive research on the production and
109 application of CTL has been carried out at the economic and technical level, making a more
110 comprehensive evaluation of FTS technology [47-53]. The findings indicate that the liquid fuels by
111 FTS provide a feasible way that is viable both technologically and economically. The advanced
112 process of CTL-based poly-generation schemes combined with co-production mode will guarantee
113 a better solution to environmental protection and resource utilization, greatly enhancing the
114 industrialization of FTS.

115 However, diesel-like fuels' high reactive autoignition characteristics make it hard to control
116 combustion rates and suffer from inhomogeneous mixture formation, so single diesel-like fuels may

117 not be the ideal choice for advanced combustion mode to realize premixed combustion operation
118 [54, 55]. Because the combustion and emission performance of ICEs are closely related to the
119 physical and chemical properties of the fuel, optimizing the fuel composition structure and
120 modifying the fuel's physical and chemical properties can meet the requirements of efficient and
121 clean combustion processes. Research institutions in various countries have invested much effort in
122 improving fuel characteristics [56-58]. The studies found that fuel with low distillate and cetane
123 number (CN) had great potential to form a homogeneous mixture and control the combustion
124 process. Therefore, it is expected that these two different fuels with opposite but complementary
125 properties can improve fuel adaptability, reaching a better compromise in the new combustion mode
126 [56]. The ideas of wide distillation fuel (WDF) have been proposed to find a way out of a difficulty
127 about the trade-off between NO_x and soot emissions in CI engines [60]. WDF is the fuel with a wide
128 distillation range from the initial boiling point of gasoline to the final boiling point of diesel.
129 Fortunately, as a petroleum product widely used in ICEs, low-reactivity gasoline can suppress
130 ignition sufficiently, and its high volatility does a favor to the homogenization of fuel-air, so gasoline
131 has been expected as a suitable choice as diesel fuel additives which is the available means to obtain
132 WDF. Diesel and gasoline blends may also change spray characteristics due to the changed physical
133 properties, finally impacting the in-cylinder mixture formation, engine combustion, and emissions
134 [61]. As the gasoline fraction increases, the density, surface tension, and kinematic viscosity of
135 blends will also decrease, and their evaporation and low-temperature fluidity are improved [62, 63].
136 Hence, diesel and gasoline blends have higher volumetric injection rates, earlier injection starts, and
137 shorter injection delays [64]. H.Fujimoto et al. confirmed that the addition of the high-volatility
138 fuels promotes the evaporation of low-volatility fuels, shortens the spray penetration distance, and

139 enlarges the spray cone angle [65]. Compared with the volatility of the fuel, the CN of fuels also
140 plays a more critical role in physical and chemical processes in the cylinder. Zhong et al.
141 experimented with the HCCI combustion quality of gasoline and diesel blend fuels, and they had
142 referred to the new combustion technology as Dieseline firstly [66, 67]. Dieseline utilizes better
143 volatility of gasoline to prepare a homogeneous mixture and high CN of diesel to be suitable for CI.
144 Han et al. [68] used diesel and gasoline blends in the LTC strategy and found that adding gasoline
145 could decrease the reliance on heavy EGR usage and combustion temperature reduction better-
146 controlling emissions. Chen et al. [69] studied adding gasoline into diesel/biodiesel blends at various
147 speeds and loads under different EGRs to reduce NO_x and soot emissions. Chaudhari et al. [70]
148 obtained clean combustion and improved efficiency with diesel-gasoline blends, and the engine
149 load-carrying capacity can be extended without decreasing the engine performance by combining
150 low and high reactivity fuels. In conclusion, it has been generally recognized that fuels with
151 properties between diesel and gasoline are feasible and potential fuels for current advanced CI
152 engines [71–73].

153 To sum up, fuel design and composition reconstruction have gradually become an essential path
154 for efficient and clean combustion of ICEs. The CTL with higher CN is blended with gasoline with
155 the resistance to autoignition and high volatility, adjusting reactivity and distillation range of
156 blended fuels. Up to now, some scholars have adjusted the properties of Fischer-Tropsch fuel by
157 adding n-butanol in different ways to achieve better combustion and emission performance [74].
158 However, adding gasoline to CTL forming WDF needs to be more comprehensively investigated,
159 and this research is essential for its practical application in the future. The objective of the present
160 study is to explore combustion performance and emission characteristics with different blending

161 ratios of CTL/gasoline blends in a CI engine, while the variation in the start of injection (SOI) along
162 with the addition of exhaust gas recirculation (EGR) permits achieving clean combustion with CTL
163 and CTL/gasoline blends. In addition, there is a close relationship between PM emissions and
164 harmful effects on human health attracting people's attention, and the structure, surface chemistry,
165 and reactivity of soot particles are very susceptible to fuel formulation and engine operating
166 parameters [75, 76], so it is necessary to measure and analyze particle characteristics. To better
167 understand the particulate matter of CTL/gasoline blends, this study measured the exhaust particle
168 size distribution (PSD) and analyzed the mass and number concentration of particles produced by
169 the WDF based on the CTL. The significance of this work is to adjust the physical and chemical
170 properties of CTL, an excellent alternative fuel, providing an alternative technical approach to
171 achieve partially premixed compression ignition.

172 **2. Experimental system and test procedure**

173 *2.1 Experimental engine and apparatus*

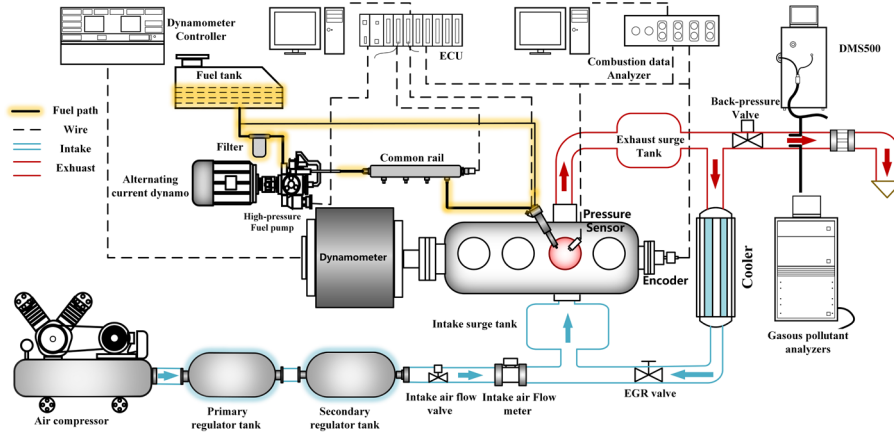
174 An inline four-cylinder CI engine equipped with high-pressure common-rail and turbocharging
175 is used as the test engine in this study. The original engine is modified into a single-cylinder CI
176 engine with controllable combustion boundary conditions to control the fuel injection and intake
177 parameters flexibly, and only the third cylinder is equipped with independent intake, exhaust, and
178 fuel injection systems. **Table 1** shows the detailed specifications of the test engine, and **Fig. 1** makes
179 clear a schematic diagram of the test platform. The test platform mainly includes a modified CI
180 engine, fuel injection control system, intake system, dynamometer, oil-water temperature control
181 system, combustion parameters analysis system, and emissions data collection system. An electronic
182 control unit (ECU, NI2106) is adopted to realize data monitor and online dynamic adjustment of

183 injection parameters. In addition, the independent intake parameters are adjusted through a self-
 184 designed simulated supercharging system, and the high-pressure air from the compressor is
 185 stabilized by a two-stage pressure surge chamber, entering the third cylinder of the test engine finally.
 186 The intake pressure of the engine is flexibly adjusted between 0 MPa and 0.3 MPa (gauge pressure)
 187 by a pressure sensor and a flow-limiting valve. The EGR system stabilizes the pressure of the
 188 exhaust surge chamber by changing the opening degree of the exhaust back-pressure valve, and then
 189 controls the EGR rate by adjusting the EGR valve.

190

Table 1. Engine specifications

Category	Properties
Geometric compression ratio	17.1
Cylinder diameter / mm	95.4
Piston stroke / mm	104.9
Connecting rod length / mm	162
The number of nozzles holes	7
Injector orifice diameter / mm	0.12
Oil jet cone angle / (°)	12
Swirl number	0.97
The shape of combustion chamber	ω



191

192

Fig. 1 Schematic diagram of experimental setup

193

The emissions measuring system is set up to collect pollutants data from the exhaust gas. NO_x concentration analyzer (Cambustion CLD 500), A fast HC analyzer (Cambustion HFR 500), and a fast CO&CO₂ analyzer (Cambustion NDIR 500) measure the concentration of NO, THC, and CO₂ separately. An electron particle spectrometer (Cambustion DMS500) is used to acquire the particle size distributions (PSDs). According to the PM diameter, the particle size is divided into three categories, namely nuclear mode particles (NMPs) (<35 nm), agglomerated particles (AMPs) (>35nm), and ultrafine particles (<100 nm). The combustion parameters acquisition and analysis system are composed of a piezoelectric sensor (Kistler 6052C) and a data acquisition system, which collects the in-cylinder pressure and other combustion parameters. For each operating point, 200 cycles of data are collected and averaged to eliminate measurement errors. The main parameters of the equipment are shown in **Table 2**.

200

201

202

203

204

Table 2. Main equipment

Category	Measuring instruments	Manufacturer	Accuracy
Dynamometer	CW260	CAMA	Torque: ± 0.5 NM Speed: ± 2 r/min

Rotary encoder	S4001	Bangman	—
Fuel flow meter	FX-100	ONO-SOKKI	± 0.12%
Air flow meter	20R100	TOCEL	± 1%
Cylinder pressure	6052C	Kistler	± 1%
CO&CO ₂	NDIR500	Cambustion	< 2% FS/hour
HC	HFR500	Cambustion	< 1% FS/hour
NO _x	CLD500	Cambustion	< 5 ppm/hour
Particle	DMS500	Cambustion	—

205 *2.2 Methodology and test conditions*

206 CTL and gasoline are selected as primary fuels in this study, and adding gasoline in different
207 proportions to the CTL to make blended test fuels. In addition, the conventional diesel is attached
208 as a reference fuel. **Table 3** compares the main physical and chemical properties of test fuels in this
209 work. The CTL used is a hydrocarbon fuel obtained from coal as a raw material through the FTS,
210 which consists of 95.8% chain alkanes, 3.4% cycloalkanes, 0.5% polycyclic aromatics and 0.3%
211 monocyclic aromatics in molar percentage. In addition, this study adopts CTL/gasoline blended
212 fuels defined as CGXX, of which the XX represents the ratio of the calorific value of gasoline to
213 the total calorific value of the fuel. For example, the blended fuel composed of 60% CTL and 40%
214 gasoline (by calorific value) is defined as CG40. Moreover, the engine operating conditions are
215 shown in **Table 4**.

216 The engine speed is maintained at 1400 r/min, and the load rate was about 60% (the indicated
217 mean effective pressure (IMEP) was about 1.0 MPa). The calorific value contained in the fuel

218 injected into the cylinder is fixed at 1704 J/cycle for all test fuels. In this experiment, the proportion
 219 of gasoline in the blended fuel is set as 20%, 40%, and 60%. The start of injection (SOI) is selected
 220 from 2 °CA before the top dead center (BTDC) to 14 °CA BTDC, and the EGR rate is set to 0% and
 221 30%. It is worth mentioning that the EGR rate is defined as the ratio of the CO₂ content in the intake
 222 and the exhaust of the engine, and the CO₂ content was measured by the exhaust gas analyzer. When
 223 the EGR rate is adjusted by controlling the mass of introduced exhaust gas, the pure air flow rate
 224 into the intake remains at 43kg/h unchanged. During the experiment, the temperature of coolant is
 225 controlled at 358±2 K.

226 **Table 3.** Main properties of tested fuels

Fuel property	CTL	Diesel	Gasoline	CG20	CG40	CG60
Density (25°C) / (kg·m ⁻³)	757.0	840.0	690	743.6	730.2	716.8
Cetane number / (CN)	75.4	52.9	13	62.92	50.44	37.96
Low calorific value / (MJ·kg ⁻¹)	43.07	42.69	42	42.87	42.64	42.42
Total Aromatics / %	≤ 0.8	≤ 3.6	0	≤ 0.64	≤ 0.48	≤ 0.32
Sulfur content / 10 ⁻⁶	0.38	3.7	~	~	~	~
Viscosity (25°C) / (mm ² ·s ⁻¹)	2.14	3.64	0.59	1.83	1.52	1.21
Theoretical air-fuel ratio	14.96	11.2	14.7	14.91	14.86	14.8

227 **Table 4.** Engine operating conditions

Category	Properties
Engine speed / (r·min ⁻¹)	1400 ± 2

IMEP / (MPa)	About 1.0
Injection pressure / (MPa)	100 ± 2
SOI / (°CA BTDC)	2-14
EGR ratio / (%)	0 and 30
Inlet air temperature / (°C)	25 ± 1
Cooling water temperature / (°C)	80 ± 1

228 For the DMS500, the concentration is expressed as a concentration size spectral density in
 229 $dN/d\log D_p$ (/cc), with units of N (/cc). It allows easy integration over any size range to give a total
 230 particle concentration, and the calculation equation is as follows:

$$231 \quad N = \int_{D_{P1}}^{D_{P2}} \frac{dN}{d\log(D_p)} d\log(D_p)$$

232 At the same time, given a size/number distribution, it is desirable to calculate in real-time a mass
 233 concentration, so the conversion equation is as follows:

$$234 \quad \text{Mass}(\mu\text{g}) = \text{Density Factor} \cdot D_p^{\text{power factor}}$$

235 For diesel engine agglomerates, research shows that the DMS500 mass calculation gives good
 236 agreement with gravimetric techniques using a density factor of $2.2 \cdot 10^{-15}$ and a power factor of 2.65.

237 **3. Results and discussions**

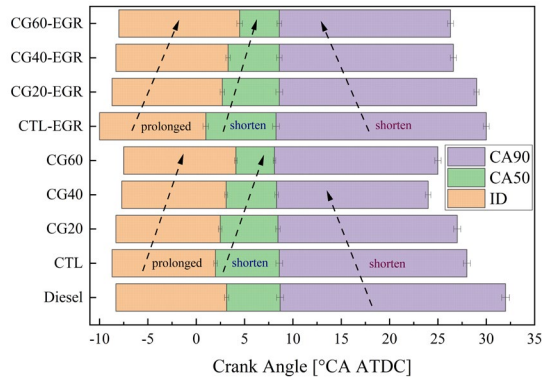
238 *3.1 Effects of CTL/gasoline blends on combustion and emissions characteristics*

239 As a potentially alternative diesel fuel, CTL is demonstrated to improve the combustion and
 240 emissions performances of the CI engine. However, the higher fuel reactivity of CTL makes itself
 241 fast auto-ignite and has poor fuel-air mixing, so it is hard to attain a higher premixed combustion
 242 mode. To optimize the feature of CTL by adjustment of physicochemical properties and fuel

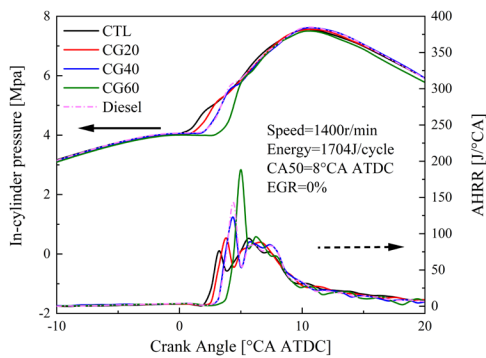
243 components, adding gasoline with low CN and high volatility to CTL forming WDF is a potential

244 and feasible solution to improve fuel adaptability to future CI engines.

245 *3.1.1 The effects of CTL/gasoline blends on the combustion performance*

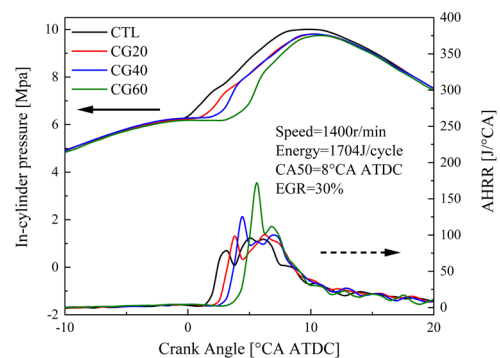


(a) Combustion phasing



(b) In-cylinder pressure and HRR with 0%

EGR



(c) In-cylinder pressure and HRR with 30%

EGR

Fig. 2 In-cylinder pressure, the HRR, and the combustion phasing of different fuels at 0% and

30% EGR rates

246 **Fig. 2** displays the variations of combustion phasing, in-cylinder pressure, and apparent heat

247 release rate (AHRR) of test fuels at different EGR rates. In order to eliminate the influence of

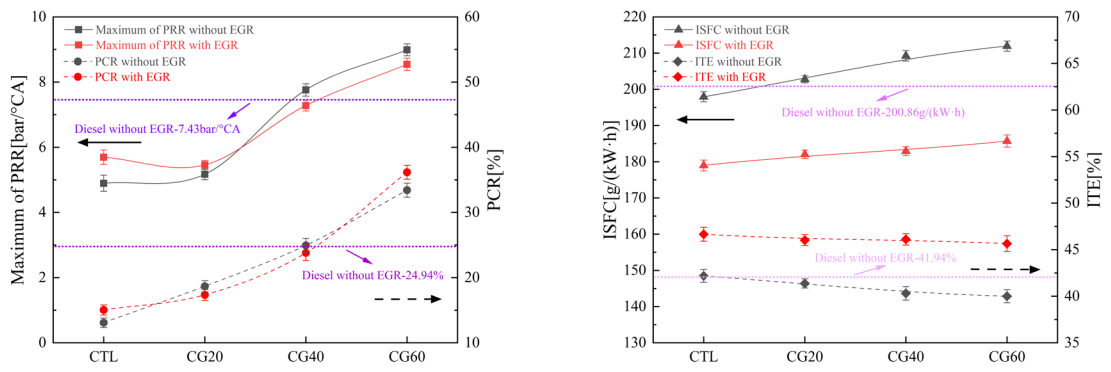
248 different combustion phasing, adjusting injection timing keeps CA50 constant at 8 °ATDC for all

249 test fuels. The CAXX represents the crank angle (CA) at which the accumulated heat release reaches
250 XX% of the entire cycle heat release. Ignition delay (ID) is defined as the time between SOI and
251 CA10, and CA10-CA90 represents the combustion duration (CD). **Fig. 2(a)** shows the combustion
252 phasing of different fuels. The higher CN and chemical reactivity indicate better ignitability, so the
253 CTL can reach the ignition conditions earlier than diesel with increases of the temperature and
254 pressure in the cylinder before combustion, making the CTL have a shorter ID than conventional
255 diesel. What also can be found is that the CD of conventional diesel is the longest. Compared with
256 the CTL, the poor reaction conditions during the later diffusion combustion process make the diesel
257 with low-reactivity burn more slowly. Even if conventional diesel has similar CN with CG40, CG40
258 has better volatility, which is beneficial to the formation of the combustible mixture in the later
259 combustion, avoiding the phenomenon of combustion tailing. It also can be seen from **Fig. 2(a)** that
260 SOI gradually advances as the gasoline proportion in the fuel decreases to maintain the same CA50
261 at a 0% EGR rate. For high CN fuels as CTL, their branched chain reaction in the low temperature
262 range, including extraction of hydrogen atoms from the fuel, oxygenation, isomerization reactions
263 and the decomposition of ketone hydro peroxide molecules, produces a large amount of active free
264 radicals such as OH, triggering a cold flame reaction at a certain temperature and leading to
265 premature ignition eventually [73]. Compared with pure CTL, the CD is gradually shortened, and
266 ID is prolonged after adding gasoline, and this trend becomes more prominent with the gasoline
267 ratio increasing. The essence of this phenomenon is that adding gasoline as an inert additive changes
268 the reaction pathway. There are weakened and slowed low-temperature reactions for WDFs
269 inhibiting OH formation reaction and reducing the exotherm in the low-temperature range, so ID is
270 prolonged by CTL/gasoline blends. Besides, due to the lowest fuel reactivity of CG60, the main

271 combustion heat release process is postponed to the stage of the expansion stroke accompanied by
272 the piston descending, slightly prolonging the CD compared to CG40.

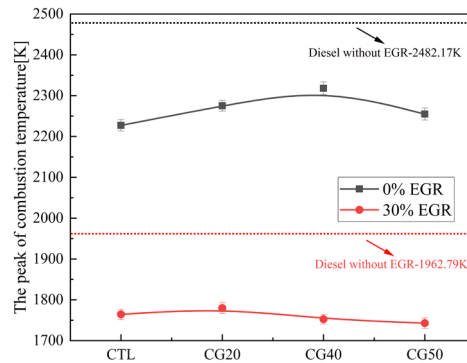
273 After introducing 30% EGR, the injection timing of pure CTL needs to be drastically advanced
274 to be consistent with CA50 without EGR, so the starting point of the heat release is also significantly
275 earlier. The sharp contrast is that the injection timing of CTL/gasoline blends only needs to be
276 advanced slightly at a 30% EGR rate to keep the same CA50 at 8 °ATDC. The above phenomenon
277 can be attributed to that EGR gas makes in-cylinder oxygen content and temperature lower during
278 the compression stroke, severely deteriorating the mixing condition of fuel and air for CTL with
279 higher CN and poor volatility. Currently, hugely advanced injection timing is beneficial to form
280 combustible mixtures to ignition for CTL. The gasoline addition with better volatility promotes
281 spray breakup, atomization, and evaporation processes of the CTL, which can effectively optimize
282 the combustion condition and reduce necessary mixing times before the start of ignition, so there is
283 a slightly advance of injection for CTL/gasoline blends at a 30% EGR. The EGR leads to a decrease
284 in the oxygen concentration, so the probability of collision between fuel and oxygen molecules
285 decreases during the chemical reaction process, inhibiting the reaction rate and prolonging the ID
286 and CD. However, CG60 minimizes the impact of EGR on CD. Under EGR operating conditions,
287 ID still prolonged with the increase of gasoline content, while CD showed the opposite trend. As
288 the gasoline proportion increases, the amount of later combustion is gradually reduced because of
289 larger premixed combustion volume shortening CD. Compared to the pure CTL with obviously
290 advanced injection timing, the CD of CG40 and CG60 was also reduced by 24.71% and 31.99%,
291 respectively. Therefore, the combustion process is not sensitive to EGR by CTL/gasoline blends; in
292 other words, and the wide distillation blended fuels are better tolerated to EGR than pure CTL.

293 Comparing to the In-cylinder pressure and AHRR curves of conventional diesel in the **Fig. 2(b)**
294 attached as a control group, there are reduced peak values of in-cylinder pressure and AHRR for the
295 CTL. In addition, since the CN of conventional diesel is close to CG40, these two fuels exhibit
296 similar combustion process. **Fig. 2(b)** shows that all test fuels have similar peaks of the in-cylinder
297 pressure when the CA50 and the total calorific value of the injected fuel remain the same without
298 EGR. However, as the gasoline content increases, the peak value of AHRR rises sharply. It can be
299 concluded that gasoline plays a role in promoting premixed combustion in the early combustion
300 stage. Due to gasoline with lower CN, increasing the gasoline ratio makes the start of heat release
301 lag behind the CTL in turn. What can be seen from **Fig. 2(c)** is that the in-cylinder pressure has
302 increased significantly after the introduction of EGR, mainly because that the EGR rate is adjusted
303 by introducing the exhaust flow while fixing the inlet flow by means of the simulated supercharge
304 system, increasing intake pressure and charge at a high EGR rate. It is necessary to significantly
305 advance the injection timing of pure CTL at a 30% EGR rate, keeping the CA50 unchanged. Hence
306 there is a significant increase in the in-cylinder pressure peak, but the peak of premixed combustion
307 still maintains the lowest level compared with CTL/gasoline blends. The changing trend of the
308 AHRRs is consistent with no EGR for four test fuels, and premixed combustion has dominated the
309 entire combustion process as the gasoline proportion increases. In conclusion, adding gasoline
310 moderately reduces the fuel cetane number of CTL extending the timescale of the mixture ignition
311 chemistry, and reduced distillation temperature and improved volatility lessening the required
312 timescale for mixture formation.



(a) Maximum of PRR and PCR at 0% and 30% EGR rates (b) ISFC and ITE at 0% and 30% EGR rates

EGR rates



(c) The peak of combustion temperature

313 **Fig. 3** Combustion characteristic of different fuels at 0% and 30% EGR rates

314 **Fig. 3** depicts the combustion characteristic of four test fuels at 0% and 30% EGR rates, including

315 that **Fig. 3(a)** shows maximum of pressure rise rate (PRR) and premixed combustion ratio (PCR),

316 **Fig. 3(b)** shows indicated specific fuel consumption (ISFC) and indicated thermal efficiency (ITE),

317 and **Fig. 3(c)** shows the peak of combustion temperature. The combustion characteristics of

318 conventional diesel fuel are given as baseline in **Fig. 3**. This paper defines the premixed combustion

319 ratio (PCR) as the ratio of the cumulative heat release of the premixed combustion endpoint (the

320 crank angle corresponding to the minimum value of the heat release acceleration) to the total

321 cumulative heat release. PRR maximums and PCRs maintain an upward trend with the increase in
322 gasoline content seen from **Fig. 3(a)**. For the pure CTL with high CN, the shortest ID keeps the
323 lowest peak of AHRR, making the smallest PCR with or without EGR. It also illustrates that creating
324 a homogenous mixture requires a very long mixing timescale, but the chemical ignition timescale
325 is very short for CTL. The addition of gasoline reduces the reactivity of the blends and promotes the
326 mixing process of fuel and air, so more combustible mixtures are produced during the longer ID due
327 to the higher gasoline content in CG40 and CG60, and these mixtures are ignited simultaneously
328 with the ignition of the CTL, considerably enhancing the PCR, and this improvement is strengthened
329 with the improved gasoline content. Thus, the faster premixed combustion speed and shorter
330 combustion duration significantly elevate the PRR maximums of CTL/gasoline blends, which is
331 also the reason for the shortening of the period during the middle and late combustion stages. It can
332 be found that PCR increases linearly with the increase of gasoline content at no EGR, and the PCR
333 of CG20, CG40, and CG60 fuels increase by 42.74%, 90.67%, and 155.50% compared with the
334 pure CTL, respectively. Moreover, there are similar cylinder pressure and AHRR curves shown in
335 **Fig. 2(b)** because diesel and CG40 have similar CN, so the maximum of PRR and PCR of these two
336 fuels are very close. However, the pure CTL's tolerance to EGR is weak, so it is needed to sharply
337 advance injection timing after introducing 30% EGR, making maximum of PRR and PCR higher
338 than no EGR. The diffusion combustion of CTL also dominates the whole combustion process of
339 CG20 due to the low gasoline content. Nevertheless, CG40 and CG60 have lower reactivity and
340 higher volatility improving the mixing process and prolonging the chemistry timescale, which
341 allows more time for fuel vaporization and consequently yields better homogenization of the fuel,
342 air, and residual gas mixture at 30% EGR. Meanwhile, the mixture will pack more EGR gas during

343 the fuel-air mixing process smoothing the combustion rate, so the PRR maximums of CG40 and
344 CG60 with obviously delayed start of combustion are lower than that of 0% EGR by 6.19% and
345 5.01% severally. ISFC and ITE show the contrary tendency as the gasoline ratio in the fuel rises
346 from **Fig. 3(b)**. It can be seen from the figure that the ISFC of CTL is lower than that of diesel,
347 because the CTL's ID is shorter improving the propensity for constant volume combustion. In
348 this study, due to the regulation of adjusting EGR, the higher intake pressure brings extra work after
349 introducing EGR, improving ITE. With or without EGR, as the proportion of gasoline in the fuel
350 increases, it can be seen that the ITE decreases and the ISFC increases gradually. It is mainly due to
351 the higher latent heat of vaporization for gasoline, and the proportion of gasoline improved leads to
352 the increase of the locally fuel-lean area leading the incomplete combustion. It is worth noting that,
353 after the introduction of EGR in this test, the ISFC of CTL/gasoline blends are closer to the pure
354 CTL.

355 **Fig. 3(c)** is a comparison of in-cylinder peak temperature for different fuels. The peak combustion
356 temperature of CTL is significantly lower than that of conventional diesel, mainly due to the large
357 proportion of diffuse combustion and almost containing no aromatic hydrocarbons with high
358 adiabatic temperature. Even if CG60 has a larger PCR, a delayed heat release process and a more
359 uniform mixture are not conducive to the generation of local high temperature, and this phenomenon
360 is especially obvious after the introduction of EGR. Since the EGR reduces the intake oxygen
361 concentration and introduces more three-atomic molecules (H_2O , CO_2), increasing the specific heat
362 capacity (SHC) of the working fluid in the cylinder, the combustion temperature drops significantly
363 at 30% EGR. Diffusion combustion of CTL is still dominated for CG20, so the peak temperature is
364 at the same level. For CG40 and CG60, the peak temperature is lower than that of pure CTL and

365 diesel. The above phenomenon is because the expansion of the fuel distillation range is conducive
 366 to the homogenization of the components in the cylinder and a large amount of exhaust gas is
 367 wrapped in the mixture, which reduces the combustion temperature and makes the combustion
 368 process softer.

369 3.1.2 The effects of CTL/gasoline blends on the emission characteristics

370 It is not difficult to see from the above discussion that the addition of gasoline to CTL is conducive to
 371 the active introduction of premixed combustion mode. Simultaneously, CTL/gasoline blends extend
 372 chemistry timescale and increase fuel-air mixing rate in favor of balance between the mixing
 373 timescale and chemistry timescale. Therefore, this section analyzes and studies the gaseous pollutants
 374 and particulates' emissions of CTL and CTL/gasoline blends.

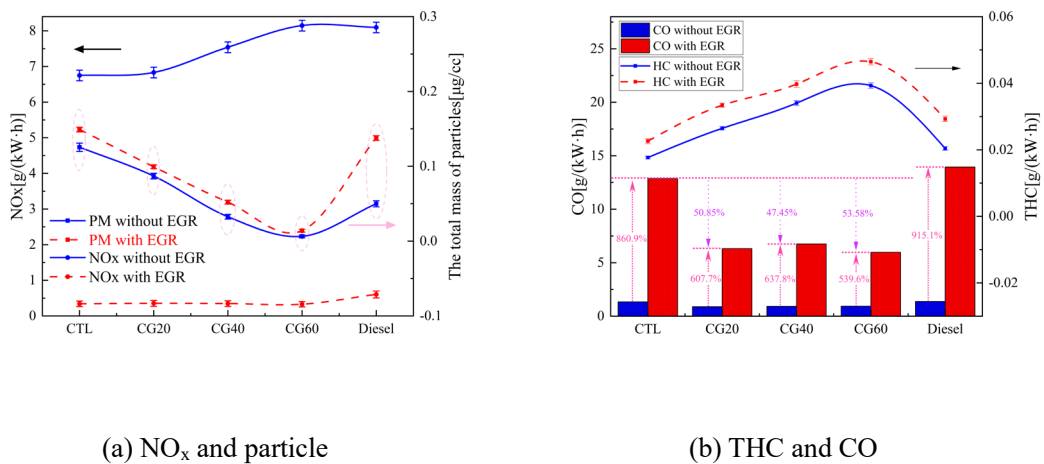


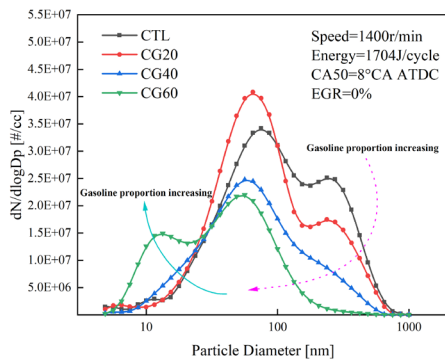
Fig. 4 Comparison of the NO_x, THC, and CO emissions for different fuels

375 **Fig. 4** displays the comparison of the NO_x, THC, and CO emissions for test fuels. It is possible
 376 to see from **Fig. 4(a)** that adding 20% gasoline does not cause a significant change in NO_x, but NO_x
 377 emissions of CG40 and CG60 rise continuously. The main reason is that the increase in gasoline
 378 ratio significantly improves the fuel and air mixing process and PCR providing more local oxygen-

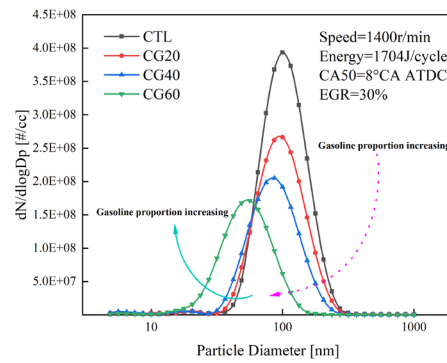
379 rich conditions and higher temperature, making for NO_x generation. Due to the highest in-cylinder
380 temperature of diesel, its NO_x emissions are close to CG60. Fortunately, 30% EGR introduced can
381 effectively suppress NO_x formation and keep NO_x emissions at low level due to lower in-cylinder
382 temperature and oxygen content slowing down combustion speed. The NO_x emissions of the four
383 test fuels are significantly lower than that of diesel with 30% EGR. CG40 and CG60 promote the
384 homogenization of fuel, air and exhaust gas, while EGR slows down the combustion rate granting
385 more time to transfer heat to cooler regions, so these factors help avoid local build-up of temperature
386 avoiding NO_x formation. For the particulates' emissions, emissions of particles masses have risen
387 after introducing EGR, and this phenomenon is very significant for diesel especially. The EGR
388 makes oxygen content and temperature decrease extending more part of combustion into the
389 expansion stroke. The nucleation mode particles formed cannot be oxidized effectively, but surface
390 addition reactions are still favored as they don't require high temperatures [74], ultimately
391 deteriorating particles' emissions. Compared to CTL, CG20, CG40, and CG60 can reduce the
392 masses of particles' emissions to 30.78%, 74.01%, and 94.97% at the condition of sufficient oxygen
393 content in the cylinder. There also is a linear decline of particles' emissions as the gasoline
394 proportion increases at a 30% EGR rate. Adding gasoline with lower reactivity into CTL can prolong
395 the ID, and gasoline with better volatility improves the atomization and evaporation process of
396 blends, promoting the quality of the fuel-air mixture during the chemical preparation period. The
397 above benefits of CTL/gasoline blends are remarkable after a drastic deterioration of combustion
398 conditions caused by the EGR. It is evident that the improvement degree of CG60 to the total mass
399 of particles is maintained at above 90% with or without EGR compared to pure CTL. Above all,
400 CTL/gasoline blends combined with EGR can break the trade-off relationship between NO_x and PM,

401 and the increase in the gasoline proportion can make particulates' emissions more resistant to EGR.

402 **Fig. 4 (b)** presents the variations in HC and CO emissions for CTL and CTL/gasoline blends. Due
403 to the introduction of EGR, the combustion temperature and oxygen concentration in the cylinder
404 decrease, resulting in a significant increase in THC and CO emissions compared to that of no EGR.
405 As shown in the figure, the THC emissions gradually increase, but CO emissions gradually decrease
406 as the gasoline blending ratio increases. As the proportion of gasoline increases, the longer ID makes
407 more fuel adhere to the cylinder wall and the locally fuel-lean regions are more easily formed, so
408 THC shows an increasing trend. The CO emissions have close relations with combustion quality,
409 which mainly depends on the fuel-air mixture formed for CI engines. After the introduction of EGR,
410 the CO emission of diesel increased by 9.15 times even exceeds the CTL, indicating that the
411 combustion of diesel is deteriorated significantly and conventional diesel has poor adaptability to
412 EGR. Fortunately, the CTL/gasoline blends can greatly improve PCR maintaining a higher
413 combustion quality and shortening CD, so the CO emissions are inhibited ultimately. CO emissions
414 are relatively low in the absence of EGR, but it increases after introducing EGR. The reduction in
415 CO of CTL/gasoline blends is maintained at above 50% compared with pure CTL. Compared with
416 no EGR operating, the decrease in in-cylinder oxygen content owing to EGR leads to an apparent
417 growth in CO emissions by 8.61 times for the pure CTL. However, CO emissions of CG20, CG40,
418 and CG60 at 30% EGR are 6.08, 6.38, and 5.40 times higher than no EGR, respectively, so this
419 upward trend of CO emissions has been alleviated by adding gasoline to CTL. The above results
420 prove again that CTL/gasoline blends can weaken the sensibility of the combustion process to the
421 lacking oxygen in the cylinder.



(a) PSD at 0% EGR



(b) PSD at 30% EGR

Fig. 5 Comparison of CTL and CTL/gasoline blends on particle size distribution at 0% and 30%

EGR

422 **Fig. 5** displays the particle size distributions (PSDs) of CTL and CTL/gasoline blends at 0% and
 423 30% EGR rates. As shown in **Fig. 5 (a)**, the PSDs of four test fuels show bimodal distribution at 0%
 424 EGR. As the proportion of gasoline increases, both peaks of the particle numbers gradually shift to
 425 smaller particle sizes. Especially, CG60 keeps the first and the second peaks at around 13nm and
 426 50nm, and the particles larger than 36.52nm decrease immensely. Due to the early flame zone
 427 chemistry has a strong influence on the total surface area of the first particle [74], a larger proportion
 428 of diffusion combustion makes more locally high-temperature and oxygen-lean regions during the
 429 combustion process, strengthening the formation of particles with the larger size for CTL.
 430 Nevertheless, CTL/gasoline blends can improve the quality of the fuel-air mixture, eliminating
 431 locally fuel-rich regions to the maximum extent, which is not conducive to the inception of particles
 432 suppressing the AMPs emissions and shifting particles towards NMPs with smaller sizes. The
 433 introduction of 30% EGR results in a unimodal distribution in the PSDs curve from **Fig. 5 (b)**, and
 434 the magnitude of the particle number increased from 10^7 to 10^8 . Introducing EGR reduces the

435 oxygen concentration and forms many oxygen-lean areas in the cylinder, deteriorating the
 436 combustion process and increasing the availability of suitable THC fragments. The fuel in some
 437 oxygen-lean areas fails to contact with oxygen fully and undergoes the process of crack, cyclization,
 438 and dehydrogenation under high-temperature conditions, finally forming carbonaceous particles
 439 with loose and porous surfaces. These porous carbonaceous particles whose specific surface area is
 440 large easily absorb THC and grow continuously and accumulate each other, generating more AMPs
 441 with larger sizes. Fortunately, as the proportion of gasoline added to CTL continues to rise, this
 442 upward trend of particulates' emissions can be effectively suppressed. The CTL/gasoline blends can
 443 not only optimize the spray characteristics, but also rely on the volatility of gasoline to form more
 444 combustible mixtures during the prolonged ID, which greatly enriches the quality of the fuel and air
 445 mixture. It is not helpful to the formation of particles inception for CTL/gasoline blends. In
 446 conclusion, as the gasoline proportion increases in the CTL/gasoline blends, the negative impact of
 447 EGR on PM has significantly been alleviated.

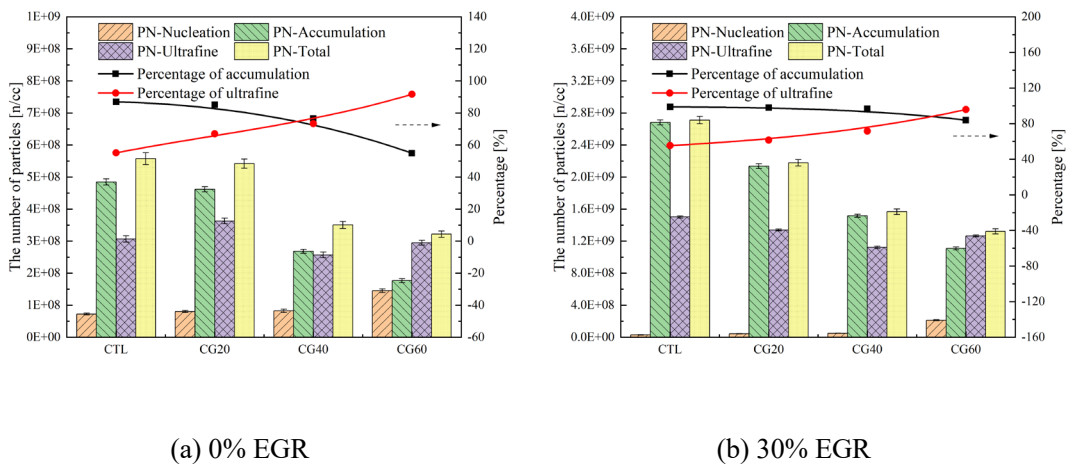


Fig. 6 Comparison of CTL and CTL/gasoline blends on different modes of particle at 0% and

30% EGR

448 **Fig. 6** manifests the comparison of CTL and CTL/gasoline blends on different modes of the
449 particle at 0% and 30% EGR. Regardless of EGR, the changes in particle characteristics show
450 consistent features as the proportion of gasoline increases. The number of total particulates and
451 AMPs both decrease significantly with the increase of the gasoline content, and the proportion of
452 AMPs has gradually diminished. As shown in **Fig. 6 (a)** at 0% EGR, the AMPs proportion in CTL
453 has reached 87.00%, but CG60 has dropped the AMPs proportion to 54.84%. Compared with CTL,
454 the total number of particles of CG20, CG40, and CG60 is lessened by 2.72%, 37.10%, and 42.24%.
455 The proportion of ultrafine particles rises with the gasoline proportion increasing, which explicates
456 that CTL/gasoline blends induce the particle size to be smaller. It can be viewed from **Fig. 6 (b)** that
457 the numbers of total particles and AMPs are closer, indicating that the AMPs have dominated the
458 entire particle size distribution at 30% EGR. Only by increasing gasoline proportion to 60% is there
459 a substantial increase in NMPs, and the ultrafine particles account for the most of total particulate
460 number. Due to the introduction of EGR, the reduced oxygen content in the cylinder precipitate
461 imperfect combustion, so the combustion in the cylinder gradually deteriorates. The possibility of
462 the formation of locally high-temperature areas with oxygen-deficient in the cylinder is increased,
463 which makes more primary particles generated, aggregated, and condensed, and more THC
464 emissions also promote the growth of particles. It is generally believed that NMPs are mainly formed
465 in the process of exhaust gas cooling and dilution, and their components are mainly soluble organic
466 matter (SOF) and some ultrafine carbon cores [75]. Therefore, the number of AMPs whose
467 adsorption of unburned HC is enhanced increases, inhibiting the NMPs generation. Eventually, the
468 number of particles has risen sharply, and the proportion of AMPs has also increased at 30% EGR.
469 CTL/gasoline blends are beneficial to the homogenization of fuel and in-cylinder charge as an

470 increase of gasoline content, so there are improved quality of fuel-air mixture and a large amount of
 471 premixed combustion, significantly restraining the formation of large-size particles. After
 472 introducing EGR, the improvement of particles' emissions by adding gasoline is more prominent.
 473 Compared with CTL, the total particle numbers of CG20, CG40, and CG60 are reduced by 19.65%,
 474 42.21%, and 51.28%.

475 *3.2 Effects of fuel injection strategy on the combustion and emissions of the CTL/gasoline blends*
 476 *engine*

477 To further study the adaptability of CTL/gasoline blends to changes in combustion phasing, this
 478 section details combustion performance and exhaust emissions characteristics of CTL and
 479 CTL/gasoline blends at different injection timings combined with EGR achieving clean combustion.

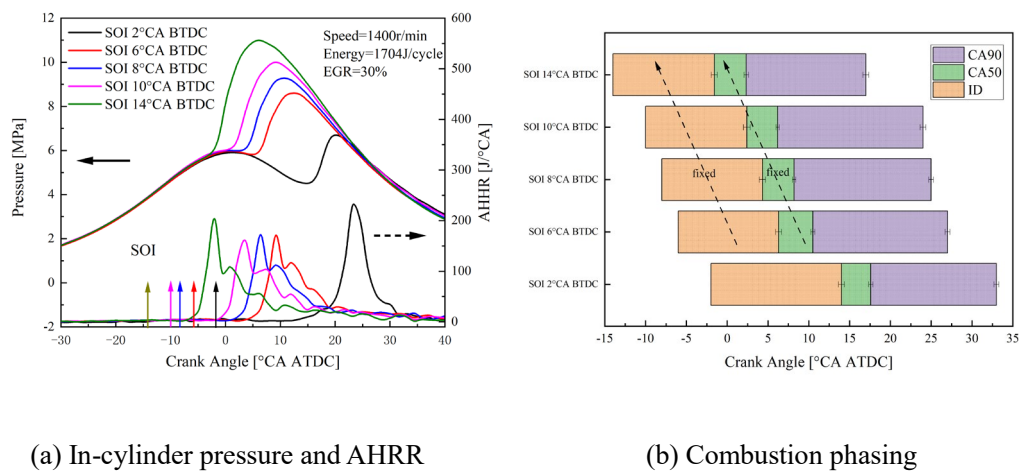
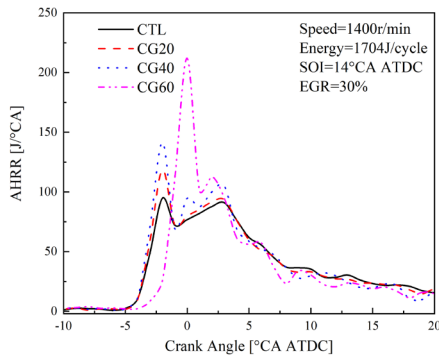


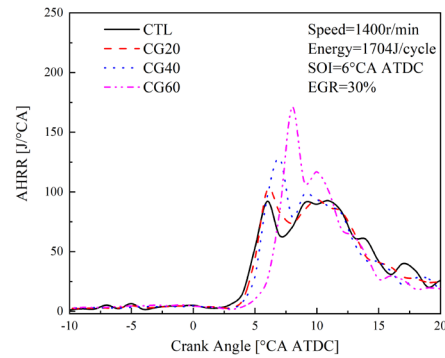
Fig. 7 Comparison of combustion characteristics at different SOI for CG60

480 **Fig. 7** shows the influence of SOI on the combustion characteristics for CG60. The research on
 481 injection timing is carried out at a 30% EGR rate, mainly to avoid tremendous combustion noise
 482 and mechanical load causing by the earlier injection timing. As shown in **Fig. 7 (a)**, when the
 483 injection timing is set to 2°CA BTDC, the combustion process is mainly postponed to the expansion

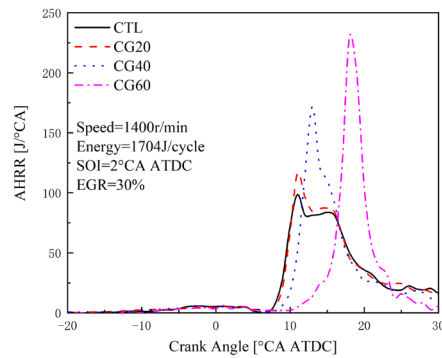
484 stroke of the CI engine, which is not suitable for the ignition of CG60 with low CN. Therefore, the
 485 start of heat release is very lagging, and the ID is greatly extended, delaying the CA50 significantly.
 486 Under the circumstances, a separation between the end of the injection and the start of the
 487 combustion is achieved, and air and fuel mix extensively prior to combustion. Hence, there is the
 488 highest peak value of AHRR whose curve tends to be unimodal, and it shows that the combustion
 489 process basically eliminates the diffusion combustion. With the continuous advance of the SOI, the
 490 maximum cylinder pressure increases because of better constant volume degrees. It also can be
 491 found from **Fig. 7 (a)** that the ID and the period of CA10 to CA50 remain almost constant, so the
 492 CA50 gradually advances linearly closer to the top dead center (TDC) with the change of injection
 493 timing from 6°CA BTDC to 14°CA BTDC from **Fig. 7 (b)**. The AHRR curves move forward and
 494 maintain the same shapes, but there is a higher peak value of AHRR as the SOI advances to 14°CA
 495 BTDC.



(a) SOI of 14 °CA BTDC



(b) SOI of 6 °CA BTDC



(c) SOI of 2 °CA BTDC

Fig. 8 Comparison of AHRRs between CTL and CTL/gasoline blends at different SOI

496 To clearly elaborate the combustion characteristic of fuels with different distillation range at
 497 various SOI, **Fig. 8** shows the comparison of AHRR between CTL and CTL/gasoline blends at SOI
 498 of 14 °CA BTDC, 6 °CA BTDC and 2 °CA BTDC. As the proportion of gasoline increases at the
 499 fixed SOI, the AHRR peak gradually becomes higher, but the start of heat release of CG60 is
 500 significantly behind mainly because the lowest fuel reactivity prolongs the ID obviously. When the
 501 SOI is relatively advanced, the start of heat release for CG20 and CG40 is basically the same as
 502 CTL, but their AHRRs have higher slopes at SOI of 14 °CA BTDC from **Fig. 9 (a)**. Because 30%
 503 EGR reduces the oxygen concentration and combustion temperature in the cylinder, which leads to
 504 the deterioration of the combustion atmosphere, but the addition of gasoline improves the formation
 505 of the combustible mixture during the preparation of chemistry, optimizing the ignition conditions
 506 and significantly increasing PCR which contributes to fast combustion speed. With the
 507 postponement of SOI, the increase in the gasoline proportion makes the start of heat release
 508 gradually delayed from **Fig. 8 (b)** and **(c)**. When the fuel injection is closer to the TDC, a relatively
 509 higher cylinder temperature and pressure are more suitable for ignition and heat release of CTL with

510 high CN, so fuel reactivity has become more prominent for the start of heat release at SOI closer to
 511 TDC. The lagging injection timing at 2 °CA BTDC makes the AHRR peak of CG40 and CG60
 512 significantly increase. At the same time, the boundary between premixed combustion and diffusion
 513 combustion of CG40 has been obscured, and it is radically close to full premixed combustion for
 514 CG60.

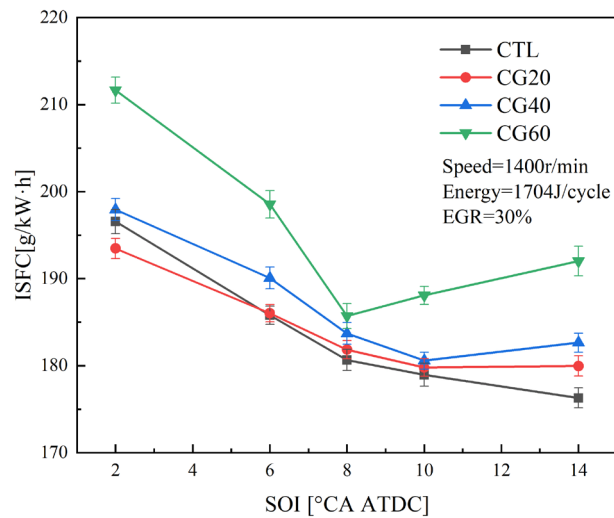


Fig. 9 Influence of SOI on the ISFC of the CTL and CTL/gasoline blends

515 According to the above discussion, SOI has a noticeable influence on the combustion
 516 characteristics of four test fuels, so the fuel economy also needs to be discussed. **Fig. 9** shows the
 517 influence of SOI on the ISFC of the CTL and CTL/gasoline blends. It can be found from the figure
 518 that as the fuel injection timing is advanced from 2°CA BTDC to 10°CA BTDC, the ISFC of the
 519 four test fuels shows a linear downward trend since early injection will cause the CA50 to approach
 520 the TDC, improving the propensity for constant volume combustion. When the fuel injection time
 521 is close to TDC, adding 20% gasoline helps to improve the quality of the mixture before the start of
 522 heat release increasing PCR, and there is no delay in combustion heat release, so the ISFC of CG20

523 is reduced by 3% at SOI of 2°CA BTDC compared with CTL. When the SOI gradually changes to
 524 14°CA BTDC, the bigger PCR results in a faster combustion rate and **maximum of PRR**, making
 525 most of the heat release maintain at the point before TDC. Therefore, an increase in the negative
 526 work that the piston must overcome decreases the fuel economy. Due to a large increase in PCR of
 527 CG60, the ISFC starts to increase at injection timing earlier than 8°CA BTDC. However, since CTL
 528 is still dominated by diffusion combustion with SOI of 14°CA BTDC, the peak heat release rate of
 529 premixed combustion is low, keeping the most combustion process after TDC, which leads to the
 530 ISFC still maintaining a decreasing trend. At the same time, it also can be found that the fuel
 531 economy of CG20 and CG40 is not significantly inferior to the pure CTL. Owing to the largest
 532 proportion of gasoline in CG60, the local area with a lower in-cylinder equivalent ratio expands,
 533 resulting in incomplete combustion. Therefore, the ISFC of CG60 is significantly higher than other
 534 fuels eventually but keeps SOI at around 8 °CA BTDC to get a better fuel economy.

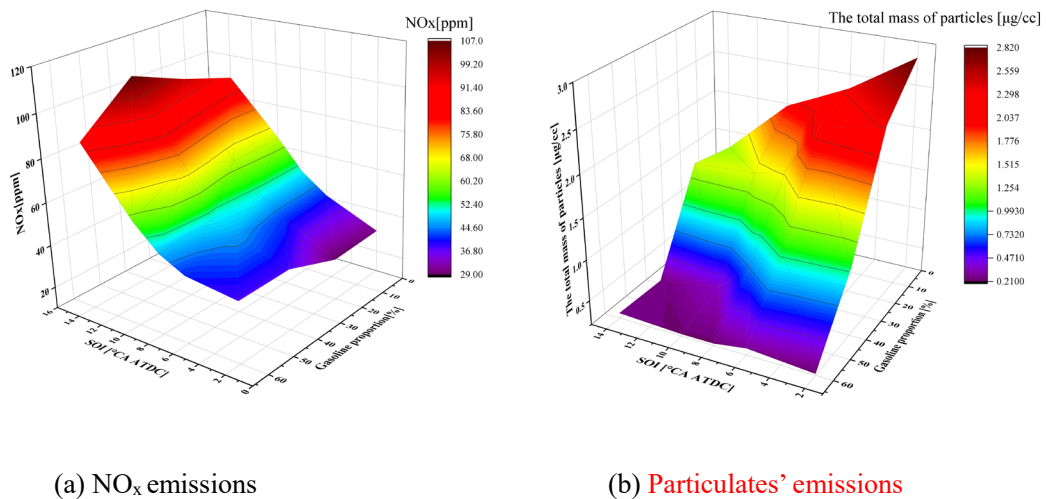


Fig. 10 Influence of injection timing on the emission characteristics of the CTL and CTL/n-butanol blends at 30%EGR

535 **Fig. 10** presents the influence of injection timing on the emission characteristics of the CTL and

536 CTL/gasoline blends at 30% EGR. The increasing NO_x emissions can be seen from **Fig. 10 (a)** with
537 the advanced injection. The reason is that the advanced injection makes the higher in-cylinder
538 pressure and maximum of PRR. NO_x emissions of CG20 and CG40 are close to the level of CTL,
539 and their NO_x emissions only show an increase when the injection timing is the most advanced (SOI
540 of 14°CA BTDC). However, the NO_x emission of CG60 is lower than that of CTL. CTL/gasoline
541 blends have a longer chemistry timescale and a better condition physical preparation before ignition,
542 and this advantage becomes more prominent as the proportion of gasoline increases. These
543 properties are conducive to the homogenization of the components in the cylinder, avoiding local
544 high temperature and smoothing combustion rate. Although CG60 has the highest PCR, its NO_x
545 emission does not increase but decreases. There is a downtrend of particulate mass as the gasoline
546 proportion increases seen from **Fig. 10 (b)**, especially CG60 reduces PM mass by above 79.53%
547 compared with pure CTL. With the advancement of SOI, the particle mass basically also shows a
548 downward trend. The main reason is that the advanced SOI and enlarged gasoline ratio will increase
549 the proportion of the combustible mixture before combustion and eliminate the excessively fuel-
550 rich area, inhibiting the generation of particles essentially. It is proved once again that the
551 CTL/gasoline blends have enhanced tolerance to EGR, and the addition of gasoline is more effective
552 than blindly advancing SOI in improving particulates' emissions at heavy EGR. It can be seen that
553 CG60 is able to decrease the total particulates' mass emissions by above 80% for all SOI compared
554 with CTL. While maintaining the same level of NO_x emissions and ISFC as the pure CTL, CG40
555 and CG60 can reduce the total particulates' mass emissions by 81.34% at SOI of 10°CA BTDC and
556 89.54% at SOI of 8°CA BTDC compared to CTL.

557 All in all, combining gasoline and control of combustion boundary conditions can minimize

558 emissions levels without deteriorating fuel economy and further break the trade-off relationship
559 between NO_x and soot.

560 **4. Conclusions**

561 Combustion processes and emission characteristics are investigated based on a modified single-
562 cylinder CI engine with flexible and adjustable control boundary parameters using CTL and
563 CTL/gasoline blends under different EGR rates. It is an attempt to change the physical and chemical
564 fuel properties of CTL by adding gasoline, meeting the needs of advanced combustion concepts and
565 realizing the integration of gasoline and diesel engines in the future CI engine. The major
566 conclusions can be summarized as follows:

567 ➤ CTL has higher CN meaning higher fuel reactivity, so the better ignitability benefits
568 shorten the ID. There is a smaller PCR due to poor fuel-air mixture quality CTL, so more
569 diffusion combustion dominates the whole combustion process. The above shortcomings are
570 fully exposed at 30% EGR. To maintain a consistent CA50 as no EGR, SOI must be greatly
571 advanced after introducing EGR. At the same time, EGR has caused a significant increase
572 in particulates' emissions of pure CTL.

573 ➤ Adding gasoline with lower CN and high volatility to CTL forms WDF, which is
574 conducive to reducing the required mixing timescale and lengthening the chemical
575 preparation timescale. Prolonged ID and improved fuel-air mixture quality bring in a higher
576 PCR increasing the peak of AHRR and fastening the combustion rate for CTL/gasoline blends.
577 In addition, the ISFC rises mildly for CTL/gasoline blends because of the incomplete
578 combustion of gasoline.

579 ➤ CTL/gasoline blends raise the PCR as gasoline proportion increases rising combustion

580 temperature, which is conducive to NO_x formation. Fortunately, the combustion temperature
581 in the cylinder was significantly reduced at 30% EGR, and the NO_x emissions of all tested
582 fuels are kept at the lowest level. Simultaneously, the inhibition effect of CTL/gasoline
583 blends on particles' emissions is evident with or without EGR, and CG60 can reduce the
584 emissions of the total particles' mass by reaching above 90% compared to CTL. Coupling
585 between EGR rate and gasoline proportion is an effective way to mitigate the trade-off
586 relationship between NO_x and particulates' emissions.

587 ➤ The change of SOI mainly affects the combustion phasing, but ID and the shapes of HRR
588 curves are not sensitive to different SOI. However, the combustion process of CG60
589 basically eliminates the diffusion combustion at SOI of 2°CA BTDC. Although NO_x grows
590 with the advance of SOI, it remains at a low level at 30% EGR. As for PM emissions, simply
591 relying on advanced SOI to remedy the aggravation of particulates' emissions caused by the
592 introduction of EGR has little effect for CTL. However, the addition of gasoline to CTL is a
593 valuable way to alleviate the deterioration of combustion and emissions caused by EGR. In
594 other words, CTL/gasoline blends make combustion performance and emission
595 characteristics have enhanced toleration to EGR. While maintaining the same level of NO_x
596 emissions and ISFC as the pure CTL, CG40 and CG60 can reduce the emissions of total
597 particulates' masses by 81.34% at SOI of 10°CA BTDC and 89.54% at SOI of 8°CA BTDC
598 compared to CTL.

599

600 **Notes**

601 The authors declare no competing financial interest.

602 **Acknowledgments**

603 This work was supported by the National Natural Science Foundation of China (Project code:
604 51476069, 51676084); Jilin Provincial Industrial Innovation Special Guidance Fund Project (Project
605 code: 2019C058-3); Jilin Province Science and Technology Development Plan Project (Project code:
606 20180101059JC); Jilin Province Specific Project of Industrial Technology Research &
607 Development (Project code: 2020C025-2); Jilin University Graduate Innovation Research Project
608 (Project code:101832020CX135).

609

610 **References**

- 611 [1] Abdul-Wahhab H A, Al-Kayiem H H, Aziz A, et al. Survey of invest fuel magnetization in
612 developing internal combustion engine characteristics. Renewable and Sustainable Energy Reviews
613 2017;79;1392-1399. <https://doi.org/10.1016/j.rser.2017.05.121>
- 614 [2] Lung H, Srna A, Chun A, et al. A Review of Hydrogen Direct Injection for Internal Combustion
615 Engines: Towards Carbon-Free Combustion. Applied Sciences 2019;9(22);4842.
616 <https://doi.org/10.3390/app9224842>
- 617 [3] Salam S, Choudhary T, Pugazhendhi A , et al. A review on recent progress in computational
618 and empirical studies of compression ignition internal combustion engine. Fuel 2020;279;118469.
619 <https://doi.org/10.1016/j.fuel.2020.118469>
- 620 [4] Kamimoto T, Bae M. High combustion temperature for the reduction of particulate in diesel
621 engines. SAE Technical Paper 880423. <https://doi.org/10.4271/880423>
- 622 [5] Kosaka H, Aizawa T, Kamimoto T. Two-dimensional imaging of ignition and soot formation

623 processes in a diesel flame. International Journal of Engine Research 2005;6(1);21-42.
624 <http://dx.doi.org/10.1243/146808705X7347>

625 [6] Desantes J M, JM García-Oliver, Antonio G, et al. Optical study on Characteristics of Non-
626 reacting and Reacting Diesel Spray with Different Strategies of Split-Injection. International
627 Journal of Engine Research 2018;1468087418773012. <https://doi.org/10.1177/1468087418773012>

628 [7] Song H, Jacobs T J. The influence of soot radiation on NO emission in practical biodiesel
629 combustion. Fuel, 2014;128:281-287. <https://doi.org/10.1016/j.fuel.2014.03.027>

630 [8] Reijnders J, Boot M, Goey P D. Impact of aromaticity and cetane number on the soot-NO_x trade-
631 off in conventional and low temperature combustion. Fuel 2016;186:24-34.
632 <https://doi.org/10.1016/j.fuel.2016.08.009>

633 [9] Imtenan S, Varman M, Masjuki H H, et al. Impact of low temperature combustion attaining
634 strategies on diesel engine emissions for diesel and biodiesels: A review. Energy Conversion &
635 Management 2014;80:329-356. <https://doi.org/10.1016/j.enconman.2014.01.020>

636 [10] Ganesh D, Nagarajan G. Homogeneous charge compression ignition (HCCI) combustion of
637 diesel fuel with external mixture formation. Energy 2010;35(1):148-157.
638 <https://doi.org/10.1016/j.energy.2009.09.005>

639 [11] Bhiogade G, Suryawanshi J G. Effects of External Mixture Formation and EGR Technique on
640 a Diesel-Fueled PCCI Engine. Journal of The Institution of Engineers (India) Series C 2020(1):1-
641 9. <https://doi.org/10.1007/s40032-020-00631-1>

642 [12] Hüseyin Aydn. An Innovative Research on Variable Compression Ratio in RCCI Strategy on a
643 Power Generator Diesel Engine Using CNG-Safflower Biodiesel. Energy 2021;231(3):121002.
644 <https://doi.org/10.1016/j.energy.2021.121002>

645 [13] Choi S, Park W, Lee S, et al. Methods for in-cylinder EGR stratification and its effects on
646 combustion and emission characteristics in a diesel engine. Fuel and Energy Abstracts 2011;
647 36(12):6948-6959. <https://doi.org/10.1016/j.energy.2011.09.016>

648 [14] Asad U, Ming Z. Exhaust gas recirculation for advanced diesel combustion cycles. Applied
649 Energy 2014;123(12):242–252. <https://doi.org/10.1016/j.apenergy.2014.02.073>

650 [15] 2020 BP Energy Outlook. BP 2020. <http://bp.com/statisticalreview>.

651 [16] Kalghatgi GT. The outlook for fuels for internal combustion engines. International Journal of
652 Engine Research 2014;15(4):383-398. <https://doi.org/10.1177/1468087414526189>

653 [17] Reitz R D. Directions in internal combustion engine research. Combustion and Flame 2013;
654 160;1-8. <https://doi.org/10.1016/j.combustflame.2012.11.002>

655 [18] Kalghatgi, Gautam. The outlook for fuels for internal combustion engines. International
656 Journal of Engine Research 2014. <https://doi.org/15.10.1177/1468087414526189>

657 [19] Song C H, Aaldering L J. Strategic intentions to the diffusion of electric mobility paradigm:
658 The case of internal combustion engine vehicle. Journal of Cleaner Production 2019;230; 898-909.
659 <https://doi.org/10.1016/j.combustflame.2012.11.002>

660 [20] Bae C, Kim J. Alternative fuels for internal combustion engines. Proceedings of the
661 Combustion Institute 2016;36(3). <https://doi.org/10.1016/j.proci.2016.09.009>

662 [21] Othman MF, Adam A, Najafi G, Mamat R. Green fuel as alternative fuel for diesel engine: A
663 review. Renewable and Sustainable Energy Reviews 2017;80;694-709.
664 <https://doi.org/10.1016/j.rser.2017.05.140>

665 [22] Kakoe A, Ghareghani A. Comparative study of hydrogen addition effects on the natural-
666 gas/diesel and natural-gas/dimethyl-ether reactivity controlled compression ignition mode of

667 operation. Energy Conversion and Management 2019;196:92-104. [https://doi.org/](https://doi.org/10.1016/j.enconman.2019.05.113)
668 [10.1016/j.enconman.2019.05.113](https://doi.org/10.1016/j.enconman.2019.05.113)

669 [23] Castro N, Toledo M, Amador G. An experimental investigation of the performance and
670 d emissions of a hydrogen-diesel dual fuel compression ignition internal combustion engine.
671 e. Applied Thermal Engineering 2019;156:660-7. [https://doi.org/10.1016/j.applthermaleng.201](https://doi.org/10.1016/j.applthermaleng.2019.04.078)
672 [9.04.078](https://doi.org/10.1016/j.applthermaleng.2019.04.078)

673 [24] Rajak U, Nashine P, Singh T S, et al. Numerical investigation of performance, combustion and
674 emission characteristics of various biofuels. Energy Conversion and Management 2018; 156:235–
675 252. <https://doi.org/10.1016/j.enconman.2017.11.017>

676 [25] Ong HC, Masjuki HH, Mahlia TMI, Silitonga AS, Chong WT, Yusaf T. Engine performance
677 and emissions using Jatropha curcas, Ceiba pentandra and Calophyllum inophyllum biodiesel in a
678 CI diesel engine. Energy 2014;69:427-45. <https://doi.org/10.1016/j.energy.2014.03.035>

679 [26] Du J, Sun W, Wang X, Li G, Tan M, Fan L. Experimental study on combustion and particle
680 size distribution of a common rail diesel engine fueled with GTL/diesel blends. Applied Thermal
681 Engineering 2014;70(1):430-40. <https://doi.org/10.1016/j.applthermaleng.2014.05.037>

682 [27] Eric D L, REN Tingjin. Synthetic fuel production by indirect coal liquefaction. Energy Sustain
683 Develop 2003;7;79e102. [https://doi.org/10.1016/S0973-0826\(08\)60381-6](https://doi.org/10.1016/S0973-0826(08)60381-6)

684 [28] Liu Z, Shi S, Li Y. Coal liquefaction technologies-Development in China and challenges in
685 chemical reaction engineering. Chemical Engineering Science 2010;65(1):12-17.
686 <https://doi.org/10.1016/j.ces.2009.05.014>

687 [29] Gao D, Ye C, Ren X, Zhang Y. Life cycle analysis of direct and indirect coal liquefaction for
688 vehicle power in China. Fuel Process Technol 2018;169:42e9.

- 689 <https://doi.org/10.1016/j.fuproc.2017.09.007>
- 690 [30] Yao X, Fan Y, Xu Y, et al. Is it worth to invest? -An evaluation of CTL-CCS project in China
691 based on real options. Energy 2019;182:920-931. <https://doi.org/10.1016/j.energy.2019.06.100>
- 692 [31] M Höök, Aleklett K. A review on coal-to-liquid fuels and its coal consumption. International
693 Journal of Energy Research 2009. <https://doi.org/10.1002/er.1596>
- 694 [32] Qin S, Chang S, Qiang Y. Modeling, thermodynamic and techno-economic analysis of coal-to-
695 liquids process with different entrained flow coal gasifiers. Applied Energy 2018; 229:413-432.
696 <https://doi.org/10.1016/j.apenergy.2018.07.030>
- 697 [33] Zhou H, Yang S, Xiao H, et al. Modeling and techno-economic analysis of shale-to-liquid and
698 coal-to-liquid fuels processes. Energy 2016;109:201-210.
699 <https://doi.org/10.1016/j.energy.2016.04.108>
- 700 [34] Williams R H, Larson E D. A comparison of direct and indirect liquefaction technologies for
701 making fluid fuels from coal. Energy for Sustainable Development 2003;7(4):103-129.
702 [https://doi.org/10.1016/S0973-0826\(08\)60382-8](https://doi.org/10.1016/S0973-0826(08)60382-8)
- 703 [35] Sudiro M, Bertu Cc O A. Production of synthetic gasoline and diesel fuel by alternative
704 processes using natural gas and coal: Process simulation and optimization. Energy 2009;
705 34(12):2206-2214. <https://doi.org/10.1016/j.energy.2008.12.009>
- 706 [36] Xu J, Yang Y, Li Y W. Recent development in converting coal to clean fuels in China. Fuel,
707 2015, 152(jul.15):122-130. <https://doi.org/10.1016/j.fuel.2014.11.059>
- 708 [37] Lacey P, Kientz J M, Gail S, et al. Evaluation of fischer-tropsch fuel performance in advanced
709 diesel common rail FIE. SAE Technical Papers, 2010. <https://doi.org/10.4271/2010-01-2191>
- 710 [38] Alleman T L. McCormick R. L. Fischer-Tropsch diesel fuels Properties and exhaust

711 missions: A literature review. Society of Automotive Engineers SP, 2003;1737:185–204. [https://doi.org/10.1016/S0140-6701\(04\)90054-9](https://doi.org/10.1016/S0140-6701(04)90054-9)

712

713 [39] S. S, Gill, A, et al. Combustion characteristics and emissions of Fischer-Tropsch diesel fuels in
714 IC engines. Progress in energy and combustion science 2011;37(4):503-523.
715 <https://doi.org/10.1016/j.peccs.2010.09.001>

716 [40] Szybist J P, Kirby S R, Boehman A L. NO_x emissions of alternative diesel Fuels:A c
717 omparative analysis of biodiesel and FT diesel. Energy & Fuels 2005;19(4):1484-1492. <https://doi.org/10.1021/ef049702q>

718

719 [41] Song C, Gong G, Song J, et al. Potential for Reduction of Exhaust Emissions in a Common-
720 Rail Direct-Injection Diesel Engine by Fueling with Fischer–Tropsch Diesel Fuel Synthesized from
721 Coal. Energy & Fuels 2012;26(1):530-5. <https://doi.org/10.1021/ef201378r>

722 [42] Dai YL, Pei YQ, Qin J, Zhang JY, Li YL. Experimental Study of Coal Liquefaction Diesel
723 Combustion and Emissions. Applied Mechanics and Materials 2013;291-294:1914-9.
724 <https://doi.org/10.4028/www.scientific.net/AMM.291-294.1914>

725 [43] Bermúdez V, Lujan J M, Pla B, et al. Comparative study of regulated and unregulated gaseous
726 emissions during NEDC in a light-duty diesel engine fuelled with Fischer Tropsch and biodiesel
727 fuels. Biomass and Bioenergy 2010;35(2):789-798. <https://doi.org/10.1016/j.biombioe.2010.10.034>

728 [44] Hao B, Song C, Lv G, et al. Evaluation of the reduction in carbonyl emissions from
729 a diesel engine using Fischer–Tropsch fuel synthesized from coal. Fuel 2014;133:115-122.
730 <https://doi.org/10.1016/j.fuel.2014.05.025>

- 731 [45] Soloiu V, Wiley J T, Gaubert R, et al. Fischer-Tropsch coal-to-liquid fuel negative temperature
732 coefficient region (NTC) and low-temperature heat release (LTHR) in a constant volume
733 combustion chamber (CVCC). Energy, 198. <https://doi.org/10.1016/j.energy.2020.117288>
- 734 [46] Armas O, Garda-Contreras R, Ramos A. Impact of alternative fuels on performance and
735 pollutant emissions of a light duty engine tested under the new European driving cycle. Applied
736 Energy 2013;107:183-190. <https://doi.org/10.1016/j.apenergy.2013.01.064>
- 737 [47] Zhou H, Yang S, Xiao H, et al. Modeling and techno-economic analysis of shale-to-liquid and
738 coal-to-liquid fuels processes. Energy 2016;109:201-210.
739 <https://doi.org/10.1016/j.energy.2016.04.108>
- 740 [48] Van Vliet OPR, Faaij APC, Turkenburg WC. Fischer-Tropsch diesel production in a well-to-
741 wheel perspective: A carbon, energy flow and cost analysis. Energy Conversion and Management
742 2009;50(4):855-76. <https://doi.org/10.1016/j.enconman.2009.01.008>
- 743 [49] Hao X, Dong G, Yang Y, Xu Y, Li Y. Coal to Liquid (CTL): Commercialization Prospects in
744 China. Chemical Engineering & Technology 2007;30(9):1157-65.
745 <https://doi.org/10.1002/ceat.200700148>
- 746 [50] Johansson D, Franck P A, Pettersson K, et al. Comparative study of Fischer-Tropsch
747 production and post-combustion CO₂ capture at an oil refinery: Economic evaluation and GHG
748 (greenhouse gas emissions) balances. Energy 2013;59:387-401.
749 <https://doi.org/10.1016/j.energy.2013.07.024>
- 750 [51] Leckel D. Diesel production from Fischer-Tropsch: The past, the present, and new concepts.
751 Energy Fuels 2009;23 (5):2342-2358. <https://doi.org/10.1021/ef900064c>
- 752 [52] Mantripragada HC, Rubin ES. CO₂ reduction potential of coal-to-liquids (CTL) process: Effect

753 of gasification technology. Energy Procedia 2011;4:2700-7.
754 <https://doi.org/10.1016/j.egypro.2011.02.171>

755 [53] Man Y, Xiao H, Cai W, Yang S. Multi-scale sustainability assessments for biomass-based and
756 coal-based fuels in China. Science of The Total Environment 2017;599-600:863-72.
757 <https://doi.org/10.1016/j.scitotenv.2017.05.006>

758 [54] Kalghatgi G, Johansson B. Gasoline compression ignition approach to efficient, clean and
759 affordable future engines. Proceedings of the Institution of Mechanical Engineers Part D Journal
760 of Automobile Engineering 2017;095440701769427. <https://doi.org/10.1177/0954407017694275>

761 [55] Kalghatgi, G. T. The outlook for fuels for internal combustion engines. International Journal of
762 Engine Research 2014;15(4):383–398. <https://doi.org/10.1177/1468087414526189>

763 [56] Liu H, Ma J, Fang D, et al. Experimental investigation of the effects of diesel fuel properties
764 on combustion and emissions on a multi-cylinder heavy-duty diesel engine. Energy Conversion &
765 Management 2018;171:1787-1800. <https://doi.org/10.1016/j.enconman.2018.06.089>

766 [57] Lu Q, Wen-Zhi L, Xi-Feng Z. Overview of fuel properties of biomass fast pyrolysis oils.
767 Energy Conversion & Management 2009;50(5):1376-1383.
768 <https://doi.org/10.1016/j.enconman.2009.01.001>

769 [58] Boudy F, Seers P. Impact of physical properties of biodiesel on the injection process in a
770 common-rail direct injection system. Energy Conversion & Management 2009;50(12):2905-2912.
771 <https://doi.org/10.1016/j.enconman.2009.07.005>

772 [59] Wang J, Yang F, Ouyang M. Dieseline fueled flexible fuel compression ignition engine
773 control based on in-cylinder pressure sensor. Applied Energy 2015;159:87-96.
774 <https://doi.org/10.1016/j.apenergy.2015.08.101>

775 [60] Wang JX, Wang Z, Liu HY. Combustion and emission characteristics of direct injection
776 compression ignition engine fueled with full distillation fuel (FDF). Fuel 2014;140:561e7. <https://doi.org/10.1016/j.fuel.2014.10.007>
777 <https://doi.org/10.1016/j.fuel.2014.10.007>

778 [61] Park SH, Youn IM, Lim YS, Lee CS. Influence of the mixture of gasoline and diesel fuels on
779 droplet atomization, combustion, and exhaust emissions characteristics in a compression ignition
780 engine. Fuel Process Technol 2013;106:392e401. <https://doi.org/10.1016/j.fuproc.2012.09.004>

781 [62] Su H P, Youn I M, Lim Y, et al. Influence of the mixture of gasoline and diesel fuels on
782 droplet atomization, combustion, and exhaust emission characteristics in a compression ignition
783 engine. Fuel Processing Technology 2013;106. <https://doi.org/10.1016/j.fuproc.2012.09.004>

784 [63] A R P, Antonio García a, A V D, et al. An experimental study of gasoline effects on injection
785 rate, momentum flux and spray characteristics using a common rail diesel injection system. Fuel
786 2012;97(7):390-399. <https://doi.org/10.1016/j.fuel.2011.11.065>

787 [64] Dong H, Wang C, Duan Y, et al. An experimental study of injection and spray characteristics
788 of diesel and gasoline blends on a common rail injection system. Energy 2014;75:513-519.
789 <https://doi.org/10.1016/j.energy.2014.08.006>

790 [65] Fujimoto H, Senda J, Kawano D, et al. Exhaust emission through diesel combustion of mixed
791 fuel oil composed of fuel with high volatility and that with low volatility. SAE Technical Papers
792 2004. <https://doi.org/10.4271/2004-01-1845>

793 [66] Zhong S, Wyszynski M L, Megaritis A, et al. Experimental Investigation into HCCI
794 Combustion Using Gasoline and Diesel Blended Fuels[J]. SAE Technical Papers 2005;2005-01-
795 3733(10):315–321. <https://doi.org/10.4271/2005-01-3733>

796 [67] Zhong S, Jin G, Wyszynski M L, et al. Promotive Effect of Diesel Fuel on Gasoline HCCI

797 Engine Operated with Negative Valve Overlap (NVO).SAE Technical Paper 2006;2006-01-0633.
798 <https://doi.org/10.4271/2006-01-0633>

799 [68] Dong, Han, Andrew, et al. Attainment and Load Extension of High-Efficiency Premixed Low-
800 Temperature Combustion with Dieseline in a Compression Ignition Engine. Energy & Fuels
801 2010;24(6):3517–3525. <https://doi.org/10.1021/ef100269c>

802 [69] Chen R H, Ong H C, Wang W C. The optimal blendings of diesel, biodiesel and gasoline with
803 various exhaust gas recirculations for reducing NO_x and smoke emissions from a diesel engine.
804 International Journal of Environmental Science and Technology 2020;17(11):4623-4654.
805 <https://doi.org/10.1007/s13762-020-02809-7>

806 [70] Chaudhari V D, Deshmukh D. Diesel and diesel-gasoline fuelled premixed low temperature
807 combustion (LTC) engine mode for clean combustion. Fuel 2020;266:116982.
808 <https://doi.org/10.1016/j.fuel.2019.116982>

809 [71] Lu X, Han D, Huang Z. Fuel design and management for the control of advanced
810 compression-ignition combustion modes. Progress in Energy and Combustion Science
811 2011;37(6):741–83. <https://doi.org/10.1016/j.pecs.2011.03.003>

812 [72] Kalghatgi GT, Hildingsson L, Harrison A, et al. Autoignition quality of gasoline fuels in
813 partially premixed combustion in diesel engines. Proceedings of the Combustion Institute
814 2011;33:3015–21. <https://doi.org/10.1016/j.proci.2010.07.007>

815 [73] Rezaei SZ, Zhang F, Xu H, et al. Investigation of two-stage split-injection strategies for a
816 Dieseline fuelled PPCI engine. Fuel 2013;107(9):299–308.
817 <https://doi.org/10.1016/j.fuel.2012.11.048>

818 [74] Soloiu V, Gaubert R, Moncada J, et al. Reactivity controlled compression ignition and low
819 temperature combustion of Fischer-Tropsch Fuel Blended with n-butanol. Renewable Energy, 2019,
820 134. <https://doi.org/10.1016/j.renene.2018.09.047>

821 [75] Wei J, Fan C, Qiu L, Qian Y, Wang C, Teng Q, et al. Impact of methanol alternative fuel on
822 oxidation reactivity of soot emissions from a modern CI engine. Fuel 2020;268:117352.
823 <https://doi.org/10.1016/j.fuel.2020.117352>

824 [76] Cadrazco M, Santamaría A, Agudelo JR. Chemical and nanostructural characteristics of the
825 particulate matter produced by renewable diesel fuel in an automotive diesel engine. Combust Flame
826 2019;203:130–42. <https://doi.org/10.1016/j.combustflame.2019.02.010>

827 [73] Peng Z, Zhao H, Tom M A, et al. Characteristics of homogeneous charge compression
828 ignition (HCCI) combustion and emissions of n-heptane. Combustion Science & Technology
829 2005;177(11):367-370. <https://doi.org/10.1080/00102200500240588>

830 [74] Natti K C, Henein N A, Poonawala Y, et al. Particulate Matter Characterization Studies in an
831 HSDI Diesel Engine under Conventional and LTC Regime. Sinéctica 2008;1(1):735-745.
832 <https://doi.org/10.4271/2008-01-1086>

833 [75] Tan P Q, Ruan S S, Hu Z Y, et al. Particle number emissions from a light-duty diesel engine
834 with biodiesel fuels under transient-state operating conditions. Applied Energy 2014;113:22-31.
835 <https://doi.org/10.1016/j.apenergy.2013.07.009>